

RESEARCH ARTICLE | JANUARY 08 2024

Laser doping of n-type 4H-SiC with boron using solution precursor for mid-wave infrared optical properties

Gunjan Kulkarni ; Yahya Bougdid ; Chandrika (John) Sugrim ; Ranganathan Kumar ; Aravinda Kar 



J. Laser Appl. 36, 012016 (2024)

<https://doi.org/10.2351/7.0001186>



CrossMark

Laser doping of n-type 4H-SiC with boron using solution precursor for mid-wave infrared optical properties

Cite as: J. Laser Appl. 36, 012016 (2024); doi: 10.2351/7.0001186

Submitted: 17 July 2023 · Accepted: 20 November 2023 ·

Published Online: 8 January 2024



Gunjan Kulkarni,^{1,2} Yahya Bougdid,^{2,3} Chandraika (John) Sugrim,⁴ Ranganathan Kumar,³ and Aravinda Kar^{1,2,a)}

AFFILIATIONS

¹Department of Electrical and Computer Engineering, University of Central Florida, Orlando, Florida 32816

²Center for Research and Education in Optics and Lasers (CREOL), The College of Optics and Photonics, University of Central Florida, Orlando, Florida 32816

³Department of Mechanical and Aerospace Engineering, University of Central Florida, Orlando, Florida 32816

⁴Naval Air Warfare Center, Aircraft Division, Patuxent River, Maryland 20670

Note: Paper published as part of the special topic on Proceedings of the International Congress of Applications of Lasers & Electro-Optics 2023.

Electronic mail: akar@creol.ucf.edu

ABSTRACT

Laser doping of n-type 4H-silicon carbide (SiC) semiconductor substrates with boron (B) using a pulsed Nd:YAG laser ($\lambda = 1064$ nm) is reported. An aqueous boric acid solution was used as a boron precursor. A simple theoretical heat transfer model was employed to select the laser processing parameters, i.e., laser power and laser-substrate interaction time, and determine the appropriate temperature to dope 4H-SiC substrates. The selected processing parameters ensured that the temperature at the laser-substrate interaction zone was below the SiC peritectic temperature to prevent any crystalline phase transformations in SiC. Fourier-transform infrared spectrometry was conducted to determine the optical properties of both undoped and boron-doped 4H-SiC substrates within the mid-wave infrared (MWIR) wavelength range (3–5 μm). Boron atoms create an acceptor energy level at 0.29 eV above the valence band in the 4H-SiC bandgap, which corresponds to $\lambda = 4.3$ μm . Boron-doped 4H-SiC substrate exhibited reduced reflectance and increased absorptance for the MWIR range. An absorption peak at $\lambda = 4.3$ μm was detected for the doped substrate. This confirmed the creation of the acceptor energy level in the 4H-SiC bandgap and, thus, doping of 4H-SiC with boron. A notable decrease in the refractive index, i.e., from 2.87 to 2.52, after laser doping of n-type 4H-SiC with boron was achieved.

Key words: laser doping, silicon carbide, MWIR optical sensor, Nd:YAG laser, refraction index

Published under an exclusive license by Laser Institute of America. <https://doi.org/10.2351/7.0001186>

I. INTRODUCTION

Silicon carbide (SiC) is a promising wide-bandgap semiconductor material known for its excellent optical, and thermophysical properties, making it suitable for various applications in harsh environments.¹ The properties of SiC include high thermal conductivity, high melting temperature, good oxidation resistance, and a high breakdown field.^{1–6} SiC exists in different crystalline structures, with the cubic (3C-SiC) and hexagonal (6H-SiC and 4H-SiC)

polytypes being the most common.⁴ Since SiC is a semiconductor material, the integration of microsensors, micro-actuators, and integrated circuits on a common substrate using microfabrication techniques is possible.⁶ Notably, 4H-SiC substrates exhibit an impressive breakdown field of 2.8 MV/cm, which is about ten times larger than that of silicon (Si).³ Consequently, 4H-SiC-based devices experience significantly lower losses compared to their Si counterparts.

Doping presents a significant challenge in the fabrication of SiC-based devices, primarily due to its hardness, chemical inertness, and very low diffusion coefficient of most impurities in SiC.⁴ Currently, epilayer doping and ion implantation are the two techniques primarily employed for doping SiC.⁷ Epilayer doping involves introducing dopants such as nitrogen (N), phosphorus (P), aluminum (Al), boron (B), and vanadium (V) during the chemical vapor deposition epitaxial growth process of SiC. On the other hand, ion implantation is the prevailing method for doping SiC.⁴ However, it has a drawback of inducing defect centers in SiC, necessitating high annealing temperatures to eliminate these defects and electrically activate the implanted species. It is worth noting that even after annealing at temperatures as high as 1700 °C, certain crystallographic defects may still persist in SiC.^{4,5} However, high-temperature annealing can result in significant surface damage due to the sublimation and redistribution of silicon.⁵

Laser doping techniques have emerged as a viable method for selectively doping SiC substrates with a variety of dopants such as gallium (Ga),^{1,2} phosphorous (P),^{3,8} nitrogen (N),^{4,6} aluminum (Al),^{4,9} chromium (Cr),^{7,10} and boron (B).¹⁰ Laser doping of SiC immersed in a variety of gaseous phase dopant species have been reported in Refs. 6–10. Bet *et al.*¹⁰ performed laser doping of intrinsic 4H-SiC and n-type 6H-SiC substrates in triethyl boron [B(C₂H₅)₃] gas using a pulsed Nd:YAG ($\lambda = 1064$ nm) laser, which resulted in the substrates exceeding the solid solubility limit of 2.5×10^{20} cm⁻³ for boron in SiC at the surface. Tian *et al.*⁴ reported the laser doping of n-type 6H-SiC using a pulsed Nd:YAG laser in trimethyl aluminum [Al(CH₃)₃] gas which exhibited an Al concentration of 2×10^{21} cm⁻³ at the substrate surface and then it dropped linearly to 1.5×10^{20} cm⁻³ within a depth of 1.1 μ m. When compared to gaseous precursors, liquid precursors have the capability to provide a higher density of dopants to the surface of the target substrate.⁸ Therefore, laser irradiation of SiC submerged in a dopant containing liquid has shown promise for selectively doping p-type and n-type SiC semiconductors. Marui *et al.*⁹ reported Al doping of n-type 4H-SiC immersed in aluminum chloride (AlCl₃) solution using a KrF ($\lambda = 248$ nm) excimer laser. This study revealed that Al atoms diffused into 4H-SiC with a concentration exceeding 10^{20} cm⁻³ at the substrate surface, while chlorine (Cl) atoms hardly penetrated the substrate. The above-mentioned studies reveal that the dopant concentration in SiC can be systematically varied by adjusting the laser processing parameters such as the number of pulse shots and laser power.⁹

Lim *et al.*¹ developed an uncooled mid-wave infrared (MWIR) detector based on laser doping of n-type 4H-SiC in triethyl gallium [Ga(C₂H₅)₃] gas. Their study revealed that gallium atoms diffused into 4H-SiC and generated an acceptor energy level of 0.3 eV in the bandgap of 4H-SiC, corresponding to an MWIR wavelength of 4.21 μ m. Fourier-transform infrared (FTIR) spectrometry analysis reported in Ref. 1 confirmed the incorporation of Ga atoms into the SiC substrate. The irradiation of Ga-doped 4H-SiC at 4.21 μ m wavelength altered the electron density, resulting in changes in its transmittance, reflectance, absorptance, and refraction index. Direct laser writing conversion, a 1064 nm laser based doping technique, enabled the production of doped tracks on SiC for n-type and p-type doping.⁵ Direct laser writing technique^{12–14} allowed the creation of conductive tracks on insulating SiC surfaces without any

need for the metallization process. By utilizing laser-induced thermal diffusion, dopant atoms could be incorporated into SiC, offering a unique and commercially viable approach for fabricating wide-bandgap semiconductor-based devices. Laser doping strategies offer an alternative to the complex, multistep traditional methods used in microelectronics manufacturing, addressing the challenges associated with ion implantation, conventional doping (thermal diffusion), and etching and metallization during the processing of wide-bandgap semiconductors.^{6,11}

Lim and Kar¹⁵ developed a thermal diffusion model to analyze the temperature-induced thermal stress that influences the depth-wise doping in SiC. This theoretical model considered various factors such as the electromagnetic field of the laser, Fickian diffusion effects, and thermal stresses resulting from localized heating caused by the laser. Bet *et al.*¹⁶ calculated the diffusivity of Cr atoms at different depths within the doped SiC substrates as a function of temperature induced by laser. This study reported maximum diffusivity of Cr atoms in SiC, reaching 6.92×10^{-12} cm²/s at 3046 K and 4.61×10^{-10} cm²/s at 2898 K for 6H-SiC and 4H-SiC, respectively.

The above-reported studies investigated laser doping of SiC with different dopants including gallium, aluminum, boron, nitrogen, phosphorous, and chromium for diverse applications such as MWIR detectors,^{1,2} nitric oxide (NO) gas sensors,² power metal-oxide semiconductor field-effect transistors,⁴ p-n junction diodes,^{3,8} interconnects,⁶ and light emitting diodes (LEDs),¹⁰ respectively. Boron out-diffusion and complete activation are problems with boron dopant incorporated into SiC by ion implantation or epitaxial doping.¹⁰ Furthermore, laser doping of SiC with excimer lasers is associated with the disadvantage of surface ablation of SiC.^{3,8,9} To overcome these issues, we developed a laser doping technique based on a pulsed Nd:YAG laser using a liquid-phase boron precursor, i.e., an aqueous solution of boric acid (H₃BO₃), to dope n-type 4H-SiC with boron. Prior to laser doping experiments, we used a simple theoretical heat transfer model to select the laser processing parameters, i.e., laser power and interaction time, and determine the corresponding temperature at the laser-substrate interaction zone for doping n-type 4H-SiC. The chosen process parameters ensured that the temperature at this interaction zone remained below the peritectic temperature of SiC, which is 2830 °C,⁷ to prevent any crystalline phase transformations in SiC during the laser doping process.

In this paper, a pulsed Nd:YAG laser has been used to dope n-type 4H-SiC substrate with boron. The laser processing parameters from the theoretical model have been chosen such that the boron dopant atoms can be incorporated into 4H-SiC substrates without causing any crystalline phase transitions in the substrate. FTIR spectrometry measurements have been used to indicate the changes in reflectance and absorptance for the boron-doped SiC substrate within the MWIR range. The absorption peak corresponding to the acceptor energy level created by the boron dopant atoms within the 4H-SiC bandgap has been determined. A substantial change in the refraction index (n) of the boron-doped sample has been detected based on the FTIR data. The hot point probe method has been used to evaluate the charge carrier type of the doped region. Photoluminescence (PL) measurement has been carried out to confirm the presence of boron acceptors

in the doped substrate. Surface profilometry has been conducted to investigate the roughness of the SiC substrate surface before and after laser doping with two different interaction times.

II. SAMPLE PREPARATION

A. SiC cleaning prior to laser doping

The process of cleaning SiC substrates before laser doping to eliminate any surface contaminants involved several steps as reported in Refs. 1 and 7. Initially, the substrates were rinsed under running tap water and then treated with de-ionized (DI) water. They were subsequently scrubbed thoroughly with soap and rinsed again with DI water. Afterward, the substrates were blow-dried with nitrogen (N_2) gas. The next step entailed immersing the substrates in a mixture of 95%–98% sulfuric acid (H_2SO_4) and 30 wt.% hydrogen peroxide (H_2O_2) in H_2O , with a 1:1 volume ratio, for 15 min. The substrates were rinsed again with DI water and blow-dried with N_2 gas. Next, the substrates were immersed in 6:1 buffered oxide etchant for 10 min to etch any native oxide of silicon that might have formed on their surfaces. The rinsing process with DI water was repeated before the substrates were cleaned with acetone, followed by methanol. A final rinse with DI water was performed, and the substrates were blow-dried with N_2 gas to complete the cleaning procedure prior to laser doping experiments.

B. Precursor solutions preparation

When it comes to laser doping techniques, dopant precursors can be present in three different phases, i.e., solid, liquid, and gaseous. However, the use of a liquid precursor for doping can offer a significant advantage in terms of the diversity of dopant species available.⁸ Liquid immersion laser doping of SiC can, therefore, greatly improve the feasibility of laser processes for the fabrication of semiconductor devices. Another benefit of using liquid precursors in laser doping is that they can deliver a higher concentration of dopant atoms to the target material's surface when compared with gas precursors.⁸ This enables more effective doping, potentially surpassing the solid solubility limit of the dopant. Consequently, the technique is highly anticipated and expected to have a significant impact on the field of semiconductor device fabrication.

In this study, n-type 4H-SiC substrates were doped with boron using a liquid-phase precursor. Boric acid (H_3BO_3) powder was used as a source of boron atoms. Saturated boric acid solution was obtained by dissolving 300 mg of H_3BO_3 powder in 5 ml of water at ambient temperature. Accordingly, 4.6 wt.% (0.75M) aqueous boric acid solution was prepared and the concentration of boron atoms in this solution was approximately $4.52 \times 10^{20} \text{ cm}^{-3}$. The concentration of boron atoms in the precursor solution was chosen to exceed the solid solubility limit of boron in SiC, which is $2.5 \times 10^{20} \text{ cm}^{-3}$.⁷ The precursor solution was stirred for 60 min at 800 rpm in ambient temperature. Figure 1 shows the transmittance spectra of 2.0, 3.0, and 4.6 wt.% boric acid solutions used for the laser doping experiments. All three boric acid solutions showed a transmittance of $\sim 91.5\%$ at $\lambda = 1064 \text{ nm}$, thereby demonstrating

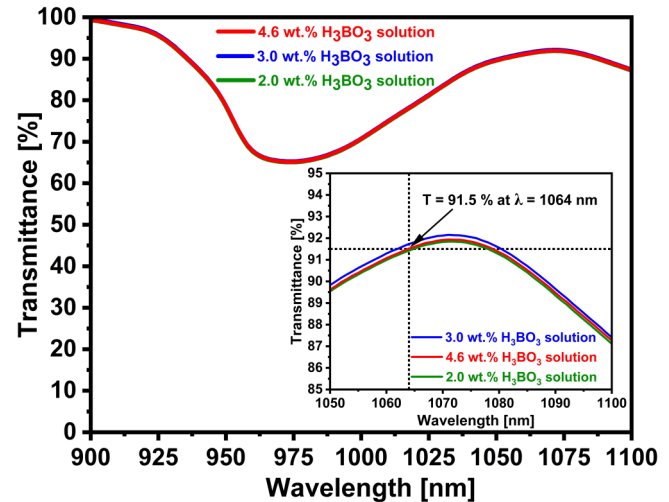


FIG. 1. Transmittance of H_3BO_3 solutions at three distinct concentrations with overlapping data lines. (Inset) Transmittance of 4.6 wt.% H_3BO_3 solution at 1064 nm wavelength.

minimal absorbance of the 1064 nm wavelength laser employed for laser doping of 4H-SiC substrates in this study.

III. LASER PROCESSING PARAMETERS SELECTION

Laser doping requires careful selection of laser processing parameters in order to achieve diffusion of dopant atoms into the SiC substrate without causing any damage to this substrate. Understanding the relationship between laser power combined with the irradiation time and the corresponding temperature at the laser-heated spot on the surface of SiC substrates is of crucial importance to achieve efficient doping. The highest temperature that can be used for laser doping prior to observing any phase transitions in SiC is 2830 °C.⁷ Figure 2 illustrates the optical properties of an undoped n-type 4H-SiC substrate at 1064 nm wavelength that were measured using an FTIR spectrometer. These measurements exhibited transmittance, reflectance, and absorbance of 18.52%, 35.13%, and 46.35% at 1064 nm wavelength, respectively.

The temperature at the laser-substrate interaction zone at any time “ t ” during the irradiation of this interaction zone by the laser beam can be expressed as follows:^{17,18}

$$T(0, t) = T_r + \left(\frac{2AP}{\kappa a} \right) \sqrt{\frac{\kappa t}{\pi}}, \quad (1)$$

where T_r is the room temperature, A is the absorbance of SiC at $\lambda = 1064 \text{ nm}$, κ is the thermal conductivity, κ is the thermal diffusivity, P is the laser power, and a is the area of interaction between the laser and SiC substrate. The values for thermal conductivity and thermal diffusivity were obtained from Ref. 11. The area on the substrate where doping occurs, $T(0, t_{\text{int}})$ is obtained from Eq. (1) at the laser-substrate interaction time, $t = t_{\text{int}} = d_{\text{LB}}/v$, where d_{LB} is the diameter of laser spot and v is the substrate velocity. The minimum

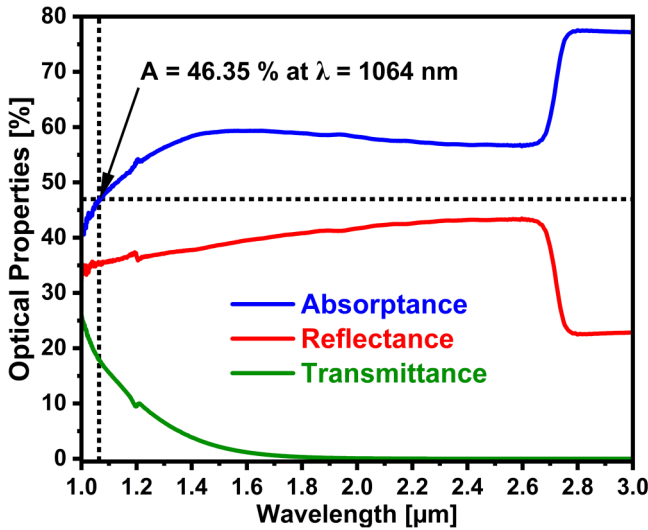


FIG. 2. Measured transmittance, reflectance, and absorptance of an undoped n-type 4H-SiC substrate. The absorptance of the substrate at 1064 nm wavelength was determined in order to be used for the theoretical calculations for selecting the laser processing parameters.

substrate velocity of 0.01 mm/s with a focused laser spot of $\sim 300\ \mu\text{m}$ diameter corresponded to a maximum laser-substrate interaction time of 30 s. The temperature on the substrate surface at the laser-substrate interaction zone is calculated as a function of laser power for different substrate velocities, as indicated in Fig. 3.

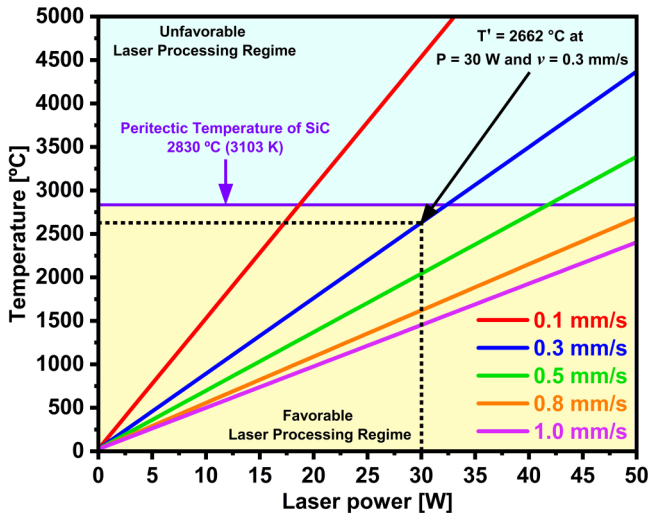


FIG. 3. Selection of laser power and scanning velocity for laser doping to avoid causing any damage to the 4H-SiC substrates. A power of 30 W at 0.3 mm/s scanning velocity that corresponds to a temperature, $T' = 2662\ \text{°C}$, was selected for our doping experiments.

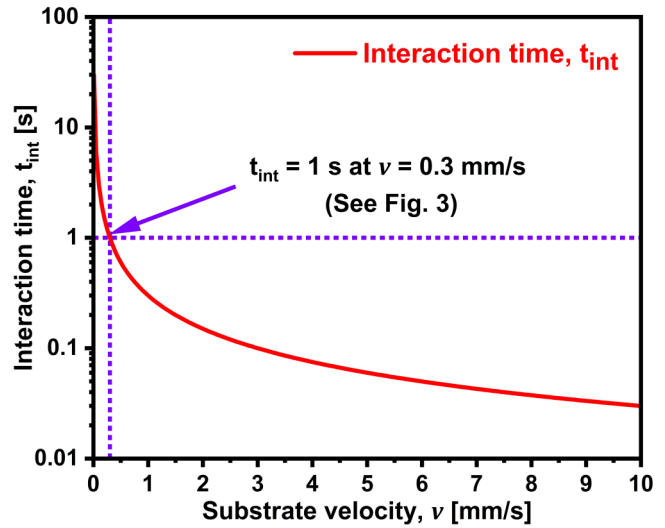


FIG. 4. Calculated laser-substrate interaction time as a function of substrate velocity.

The dependence of laser-substrate interaction time on substrate velocity for a laser spot of $\sim 300\ \mu\text{m}$ diameter has been illustrated in Fig. 4.

The theoretical model, as depicted in Figs. 3 and 4, indicates that a power of 30 W at 0.3 mm/s velocity, with a laser spot size of $\sim 300\ \mu\text{m}$, results in a temperature of 2662 °C at the laser-substrate interaction zone. Figure 3 illustrates that these laser processing parameters were selected to maintain the temperature at the laser-substrate interaction zone well below the peritectic temperature of SiC, thus preventing any damage or phase shifts in the SiC substrates.⁷ Furthermore, it is important to note that using the same laser spot size of $300\ \mu\text{m}$ with a power exceeding 30 W or a scanning velocity less than 0.3 mm/s leads to boiling of the precursor solution, causing undesirable splashing and substrate shaking.

IV. EXPERIMENTAL PROCEDURE

A. Laser doping experiment

A 150 mm diameter n-type 4H-SiC wafer (Si-face 4° off-axis, $\pm 0.5^\circ$) of thickness $350 \pm 25\ \mu\text{m}$ was purchased from II-VI Advanced Materials Inc. and laser cut to produce $10 \times 10\ \text{mm}^2$ square substrates. The nitrogen dopant concentration and resistivity of the n-type 4H-SiC wafer was $\sim 10^{16}\ \text{cm}^{-3}$ and $0.02\ \Omega\ \text{cm}$, respectively. Figure 5 illustrates the experimental setup used for laser doping of 4H-SiC substrates with boron in this study. Nd:YAG laser ($\lambda = 1064\ \text{nm}$) provides lower photon energy and a deeper dopant penetration depth compared to the excimer lasers (ArF: $\lambda = 193\ \text{nm}$, KrF: $\lambda = 248\ \text{nm}$, and XeF: $\lambda = 351\ \text{nm}$) because of the higher surface temperature and heat conduction to larger depth into the substrate.⁴ Higher repetition rate and longer pulse width in Nd:YAG laser treatment allow the substrate surface to remain at a higher temperature for a longer duration (irradiation time) in

08 January 2024 14:36:20

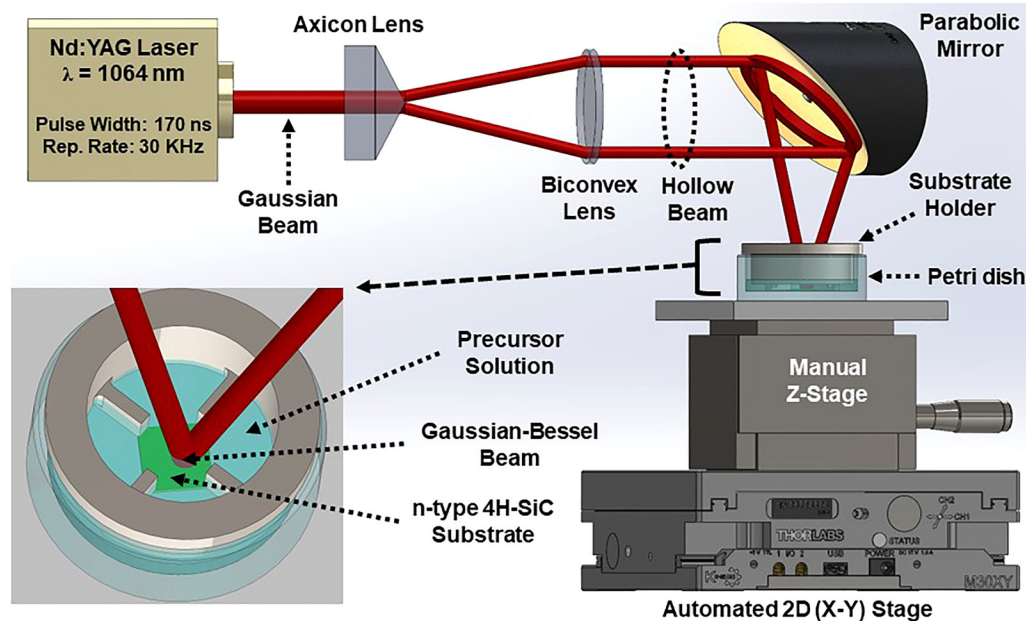


FIG. 5. Schematic illustration of the optical setup used for laser doping.

comparison to excimer laser treatment. In our study, the selective-area laser-induced diffusion of boron into n-type 4H-SiC substrates was conducted utilizing a pulsed Nd:YAG ($\lambda = 1064$ nm) laser. The pulse width and repetition rate for the laser system were set to 170 ns and 30 KHz, respectively. The original Gaussian beam from the laser source was converted into a cylindrical annular beam of uniform radial irradiance distribution through an arrangement of an axicon lens and a biconvex lens; respectively, and the annular beam was focused using a gold-coated parabolic mirror to form a hollow laser cone. At the focal point of the parabolic mirror, i.e., the apex of the cone, the original Gaussian beam transformed to a Gaussian-Bessel beam with an irradiance distribution different from the typical Gaussian irradiance distribution. The interaction between the laser light, precursor solution, and 4H-SiC substrate occurred at the apex of the cone. The focused laser spot was set at ~ 300 μm diameter. The substrate was moved underneath the laser beam by operating the automated 2D (X-Y) stage. Before the experiment, the 2D (X-Y) stage was programmed to control the motion of the substrate to achieve laser beam scanning over an area of 6×6 mm^2 . The laser beam was scanned for 6 mm in the x-direction, then the substrate was moved in the y-direction and scanning was repeated in the x-direction.

Additional vacancies in SiC could be created by laser irradiation because of stress effects such as thermal expansion, laser-induced shock waves, and vibrational excitations.¹⁹ Boron dopant atoms can diffuse into the 4H-SiC substrate through these vacancies. Cleaned 4H-SiC substrate was placed in a petri dish beneath the laser beam. A customized substrate holder was used to prevent any substrate movement during the laser-substrate interaction and give more stability to the laser doping process. The substrate was

irradiated with 30 W laser power at 0.3 mm/s substrate velocity at ambient temperature to out-diffuse several nitrogen atoms and create vacancies on the substrate surface. Doping was carried out on the Si-face of the off-axis n-type 4H-SiC substrate. A substrate velocity of 0.3 mm/s was selected that corresponded to a laser-substrate interaction time of 1 s for a single laser scan (see Fig. 4). Thereafter, the substrate was covered with 4.6 wt. % boric acid (precursor) solution. A thick layer of precursor solution covering the substrate may absorb the laser light and affect the doping process. To avoid such an issue, the thickness of the precursor solution layer covering the substrate was carefully adjusted to ~ 100 μm above the SiC surface.

The laser irradiation of an n-type 4H-SiC substrate immersed in boric acid solution with pulsed Nd:YAG laser at ambient temperature led to the generation of boron atoms due to thermal decomposition of the precursor solution at the laser-heated spot. These boron atoms subsequently diffused into the 4H-SiC substrate. The laser heating of the substrate and the diffusion of boron atoms into the substrate occurred simultaneously during the laser doping process. The SiC substrate experiences non-isothermal conditions characterized by rapid localized heating and quick cooling. This enables the substrate temperature at the interaction zone to reach a high temperature of 2662 °C within a very short time frame without surpassing the SiC peritectic temperature. The rapid heating induces one-way diffusion of boron dopant atoms into the 4H-SiC substrate while the laser pulse is on. Conversely, when the laser pulse is off, the boron atoms remain stationary, held in their positions by the rapid cooling process. These immobilized boron atoms resume their downward diffusion once the laser pulse is on. To achieve p-type doping, a laser beam of power 30 W was

scanned over the substrate by moving the substrate at 0.3 mm/s in the x and y directions using an automated 2D (X–Y) stage to cover an area of $6 \times 6 \text{ mm}^2$ on the substrate surface. After laser doping, the substrate was cleaned using a 45 wt. % potassium hydroxide (KOH) solution. Subsequently, it was rinsed with acetone, followed by methanol, and then rinsed with DI water before being blow-dried with N_2 gas. With no further processing required, the boron-doped 4H-SiC substrate was deemed suitable for MWIR detector applications.

B. Hot point probe measurement to demonstrate the presence of p-type charge carriers due to p-type doping

The undoped (n-type) 4H-SiC substrate, being doped with nitrogen, consists of electrons as the majority of charge carriers. As boron acts as a p-type dopant for SiC, boron-doped 4H-SiC consists of holes as the majority of charge carriers. Doping the undoped (n-type) 4H-SiC substrate with boron converts it to p-type.

The hot point probe measurement was carried out on the boron-doped SiC substrates to validate p-type doping by measuring the presence of p-type charge carriers (holes) within the doped substrates. Figure 6 presents a schematic illustration of the hot point probe technique, which provides a simple way to differentiate between the undoped (n-type) and boron-doped (p-type) 4H-SiC substrates by identifying the majority of charge carrier type in them by using a soldering iron and standard voltmeter. The hot point probe technique operates on the principle that, within a semiconductor, the thermally excited charge carriers diffuse away from the hot probe to the cold probe, creating a potential difference. Two probes, a hot probe and a cold probe, connected to a sensitive voltmeter, were utilized in this method. The hot probe, formed with a soldering iron, was connected to the positive

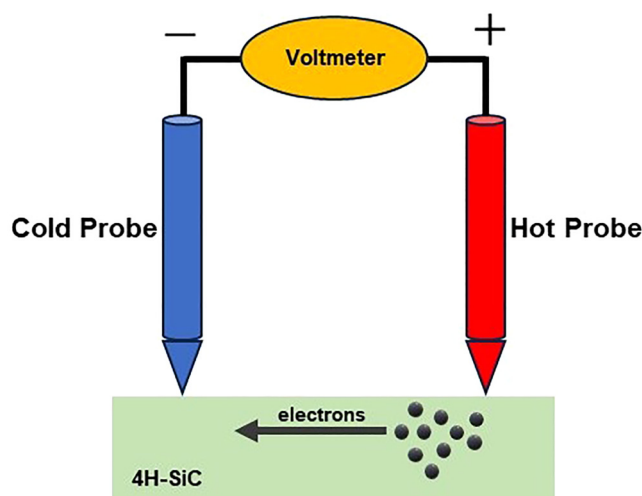


FIG. 6. Schematic representation of hot point probe technique for majority of charge carrier type analysis.

terminal of the voltmeter, while the cold probe was connected to the negative terminal. The n-type and p-type 4H-SiC substrates showed positive and negative voltages, respectively. This change in the sign polarity of the voltage reading was because the region surrounding the hot probe became filled with minority charge carriers and vice versa at the cold probe.¹⁸

V. RESULTS AND DISCUSSION

Our study presents a laser doping technique to dope n-type 4H-SiC with boron using a pulsed Nd:YAG laser. Boron is a p-type dopant in 4H-SiC wide-bandgap semiconductors. When 4H-SiC is doped with boron, the boron dopant atoms create an acceptor level of energy, $E_a = 0.29 \text{ eV}$, above its valence band.²⁰ The acceptor level comprises vacancies (holes) that can be filled by electrons when the electrons in the valence band are excited by incoming electromagnetic radiation. E_a is related to an electromagnetic radiation of wavelength, $\lambda = 4.3 \mu\text{m}$, based on the relation, $E_a = (h \times c)/\lambda$, where h is the Planck constant and c is the speed of light.¹⁰ After doping 4H-SiC with boron, an incident electromagnetic radiation of this specific wavelength excites a certain number of electrons per unit volume (N_e) to transition from the valence band to the acceptor energy level. An increase in N_e at the acceptor level changes the refractive index (n) and absorption index (k) of the doped 4H-SiC.^{21–23} The reduction or increase in the refractive index depends on the wavelength of the electromagnetic radiation and on the natural frequency of the electrons in the semiconductor material.^{21–23} Fresnel's equation from Ref. 18 [see Eq. (7)] provides a relationship between reflectance, n and k . Thus, increased N_e at the acceptor level affects the transmittance (T) and reflectance (R),^{18,21–23} resulting in an absorptance, $A = 1 - T - R$, in the B-doped SiC. The absorption peak at $4.3 \mu\text{m}$ is due to the strong absorption of the electromagnetic radiation of this wavelength by the valence band electrons to transition to the acceptor level created by the boron dopant atoms.

The optical properties of the undoped and boron-doped 4H-SiC substrates were characterized within the MWIR range using a Perkin Elmer Spectrum-2 FTIR spectrometer as shown in Figs. 7–9. The mathematical analysis of the optical properties for determining the change in refraction index is for normal incidence angle. It can be noticed that after laser doping, transmittance and reflectance were reduced whereas the absorptance increased over the entire MWIR range. The boron dopant atoms alter the absorptance characteristics of the undoped 4H-SiC substrate by enhancing the absorption peak at $\lambda = 4.3 \mu\text{m}$ corresponding to 0.29 eV energy of photons. Figure 8 illustrates the measured absorptance of undoped and boron-doped substrates at $4.3 \mu\text{m}$ wavelength to be 53.62% and 60.43%, respectively. These FTIR measurements demonstrated the difference in the optical properties of the substrate before and after doping and, hence, they verified the creation of the acceptor energy level within the 4H-SiC bandgap and doping of the 4H-SiC substrate with boron.

The measured transmittance, reflectance, and absorptance from the undoped and boron-doped substrates in the MWIR range are used to determine the absorption coefficient (α) using the

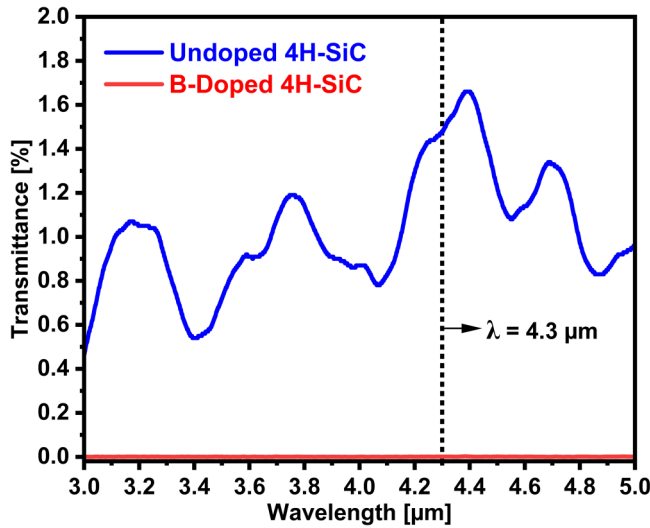


FIG. 7. Measured transmittance spectra of the undoped and boron-doped 4H-SiC substrates.

following relation:²⁴

$$\alpha = \frac{1}{d} \ln \left(\frac{1-R}{T} \right), \quad (2)$$

where d is the thickness of the 4H-SiC substrate, T is the transmittance, and R is the reflectance. The absorption coefficient (α) is

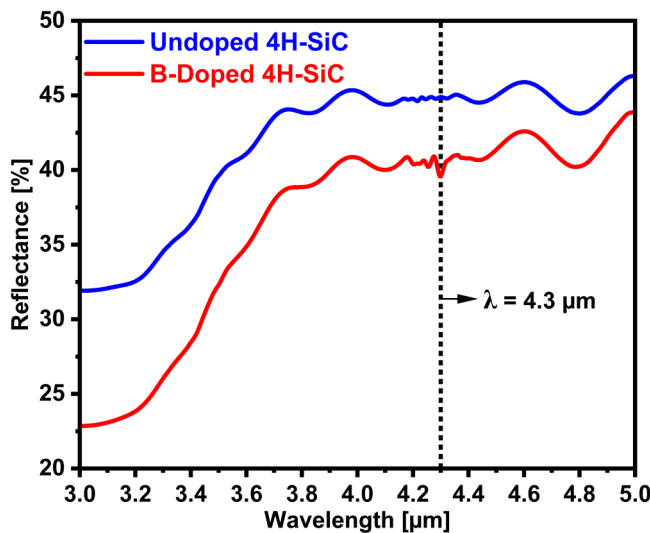


FIG. 8. Measured reflectance spectra of the undoped and boron-doped 4H-SiC samples.

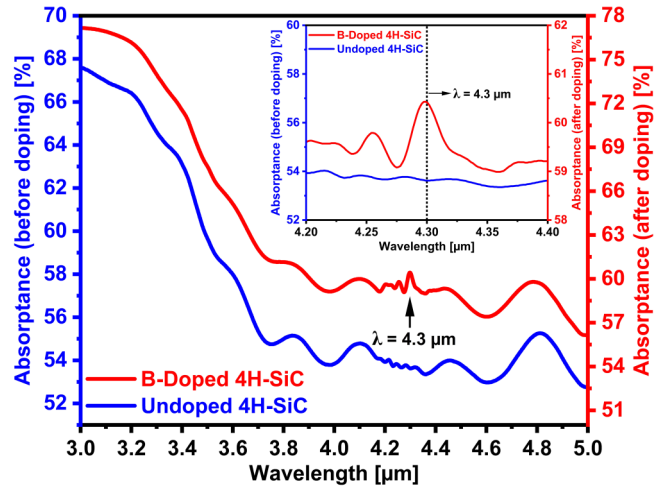


FIG. 9. Absorbance spectra of the undoped and boron-doped substrates. The absorption peak obtained at $4.3 \mu\text{m}$ wavelength is shown as an inset.

related to absorption index (k) by the following formula:²⁴

$$\alpha = \frac{4\pi k}{\lambda}. \quad (3)$$

Figures 10 and 11 show the variation of the absorption coefficient and absorption index (k) with wavelength before and after doping. Based on the data in Fig. 10, the values of the absorption coefficients before and after doping at $4.3 \mu\text{m}$ wavelength were calculated to be 10.95 and 36.09 mm^{-1} , respectively. Using the

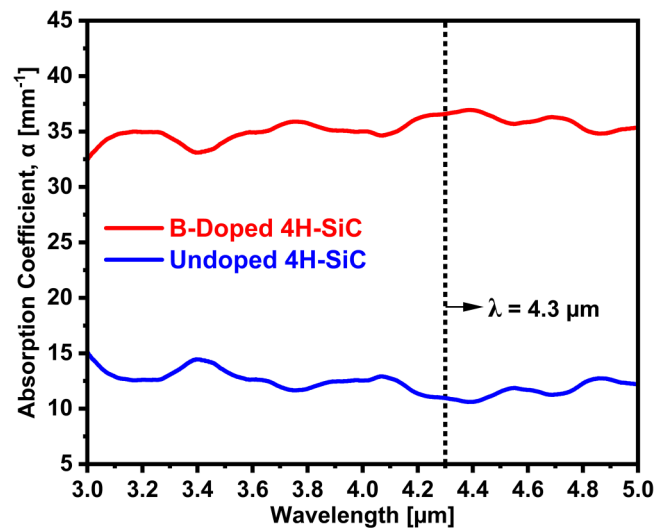


FIG. 10. Absorption coefficient of undoped and boron-doped substrates as a function of wavelength.

08 January 2024 14:36:20

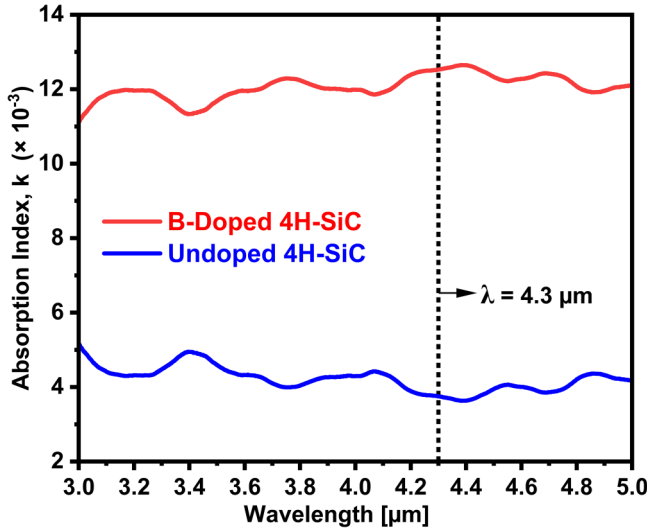


FIG. 11. Calculated absorption index of undoped and boron-doped substrates as a function of wavelength.

absorption coefficient data, the absorption index before and after doping was calculated to be 3.75×10^{-3} and 12.53×10^{-3} , respectively. The doped sample exhibits higher absorption coefficient and absorption index values in contrast to the undoped sample.

Multiple reflections in a single absorbing layer from Ref. 25 were used to derive the relationship between reflectivity (ρ) and reflectance (R) as follows:

$$R = \rho + \left[\rho(1 - \rho)^2 e^{-2\alpha t} \right] + \left[\rho^3(1 - \rho)^2 e^{-4\alpha t} \right] + \left[\rho^5(1 - \rho)^2 e^{-6\alpha t} \right] + \dots, \quad (4)$$

$$R = \rho + \rho(1 - \rho)^2 e^{-2\alpha t} \left\{ 1 + \rho^2 e^{-2\alpha t} + \rho^4 e^{-4\alpha t} + \dots \right\}. \quad (5)$$

The sum of infinite geometric series in Eq. (5) can be expressed as follows:

$$R = \rho + \frac{\rho(1 - \rho)^2 e^{-2\alpha t}}{1 - \rho^2 e^{-2\alpha t}}. \quad (6)$$

Using Eq. (6), the reflectivity was calculated for the undoped and boron-doped substrates. As the transmittance of both substrates is significantly less for the MWIR range, our calculations showed that the reflectivity is approximately equal to the corresponding reflectance values, i.e., $\rho = R$, for each substrate. The refractive index (n) values for both the undoped and boron-doped substrates were determined at different wavelengths using the

well-known Fresnel's formula¹⁸

$$R = \frac{(n - 1)^2 + k^2}{(n + 1)^2 + k^2}. \quad (7)$$

Figure 12 illustrates the refractive index (n) as a function of wavelength (λ) for both the undoped and boron-doped samples. On the other hand, Fig. 13 depicts the deviation in refractive index (Δn). The refractive index of the undoped 4H-SiC substrate varies approximately from 2.1 to 3.0 in the MWIR wavelength range (see Fig. 12). The considerable decrease in refractive index of the boron-doped substrate across the entire MWIR wavelength range can be attributed to the creation of acceptor energy level within the bandgap of 4H-SiC by the introduced boron dopant atoms. The refractive indices of the undoped and boron-doped substrates were determined to be 2.873 and 2.517 as shown in Fig. 12, respectively, at the $4.3 \mu\text{m}$ wavelength. These refractive index values correspond to a deviation of $\Delta n = 0.356$ for the sample. Our finding is in good agreement with previously published research studies.^{1,15}

A method for doping 4H-SiC with boron at ambient temperature has been demonstrated in order to fabricate a detector for the MWIR wavelength of $4.3 \mu\text{m}$. Our results demonstrated that the boron atoms were incorporated into the SiC semiconductor. The doped 4H-SiC substrate could be used as an MWIR detector without any further processing, e.g., etching or thermal annealing. Based on our laser doping experiments, multiwavelength MWIR detectors can also be manufactured on a single substrate by selectively doping the SiC substrate with different dopants using the same optical setup, as reported by Kar *et al.* in Refs. 1 and 15. Our study demonstrated that two physical phenomena, i.e., thermal decomposition of the precursor solution at the laser-heated spot and laser-induced diffusion of boron atoms into the SiC substrate occurred simultaneously during laser

08 January 2024 14:36:20

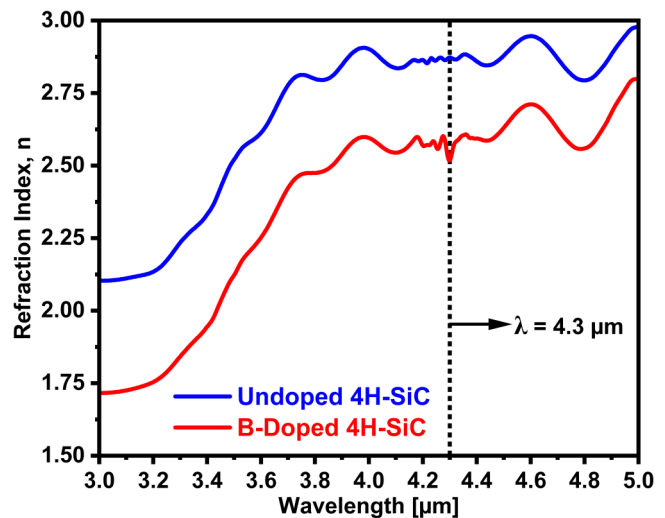


FIG. 12. Refractive index as a function of wavelength for both the undoped and boron-doped 4H-SiC substrates.

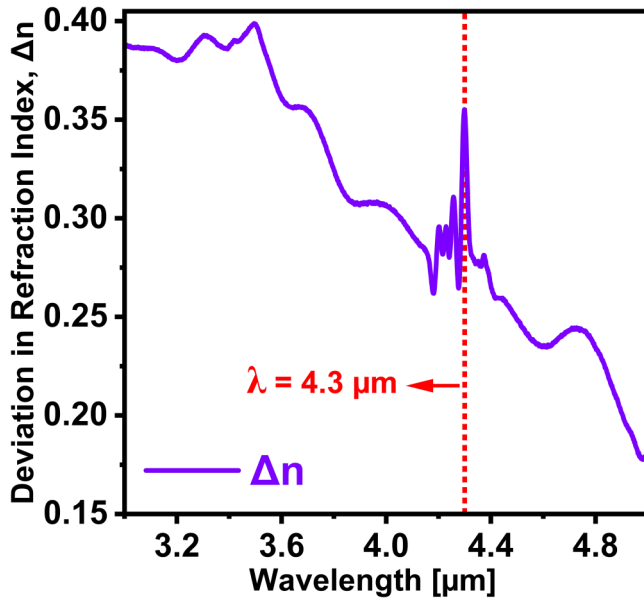


FIG. 13. Deviation in refraction index between the undoped and boron-doped 4H-SiC substrates as a function of wavelength.

doping. The FTIR spectrometry measurements of the doped SiC substrates revealed a sharp peak at 4.3 μm; corresponding to 0.29 eV, with 60.43% absorptance, which is higher than the 53.62% absorptance of the undoped substrate, respectively, as shown in Fig. 9. FTIR analysis in Fig. 9 showed additional peaks in the absorptance graphs, and these peaks could be attributed to the presence of defects or impurities within the SiC substrate.¹ Excitation of the doped substrate with an irradiation wavelength of 4.3 μm modifies the electron density, leading to a substantial variation in the refraction index and absorption index compared to those of the undoped substrate.

The bandgap of the undoped 4H-SiC substrate was estimated near the fundamental absorption edge using Tauc's relation²⁵

$$(\alpha h\nu)^{1/2} = A(h\nu - E_g)^m, \quad (8)$$

where α is the absorption coefficient, $h\nu$ is the photon energy, A is a constant (characteristic parameter for this transition), h is Planck's constant, ν is the frequency of incident light radiation, E_g is the optical bandgap energy, and m is the parameter that characterizes the transition process involved. The parameter m takes a value of 2 for direct bandgap semiconductors whereas it is taken as 1/2 for indirect bandgap semiconductors. SiC being an indirect bandgap semiconductor, m takes the value of 1/2. Tauc's relation plot, $(\alpha h\nu)^{1/2}$ versus $h\nu$, for the undoped 4H-SiC substrate is presented in Fig. 14. The optical bandgap of the substrate was evaluated by extrapolating the straight-line segment of $(\alpha h\nu)^{1/2}$ versus $h\nu$ graph to intercept the energy axis. The bandgap energy of the undoped 4H-SiC was determined to be 3.227 eV, which is similar to that reported in Refs. 6 and 10.

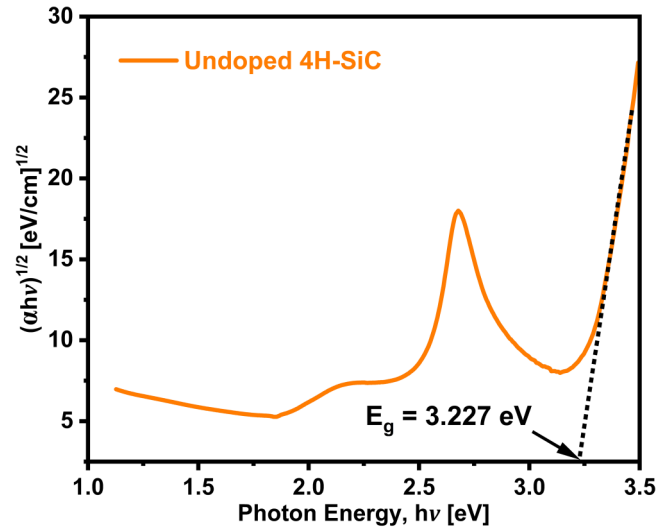


FIG. 14. Optical bandgap energy of the undoped 4H-SiC calculated using Tauc's relation (Ref. 25).

The PL spectra of the undoped (4H-SiC:N) and boron-doped 4H-SiC (4H-SiC:B) substrates are shown in Fig. 15. The PL measurements were carried out at ambient temperature with an excitation wavelength of 355 nm to verify the presence of boron atoms in the 4H-SiC substrate. The PL spectrum of 4H-SiC:B is attributed to nitrogen-to-boron donor-acceptor pair transitions (DAP, N-B) and it exhibited a broad phonon peak centered at ~2.4 eV ($\lambda = 515.5$ nm).²⁰ This broad peak signifies the intense green

08 January 2024 14:36:20

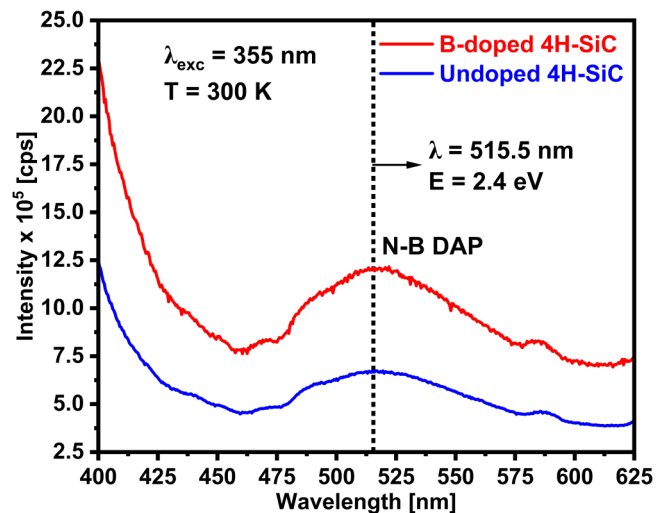


FIG. 15. PL measured at ambient temperature for the undoped and boron-doped substrates. The broad phonon peak is obtained at $\lambda = 515.5$ nm, which corresponds to an energy of 2.4 eV.

emission from the doped 4H-SiC substrate. The PL spectrum due to N/B donor–acceptor pairs in Fig. 15 confirmed the presence of N donors and B acceptors, thus demonstrating boron doping of the investigated substrate.

For the majority of charge carrier type analysis using the hot point probe technique (see Sec. IV B), the hot probe (soldering iron) was heated to a temperature of $\sim 200^\circ\text{C}$ whereas the cold probe was at ambient temperature.²⁶ When the two probes contacted the undoped (n-type) 4H-SiC sample, +5 V was registered. Conversely, -6 V was registered for the boron-doped (p-type) 4H-SiC sample. The negative potential registered on the voltmeter for the boron-doped 4H-SiC sample validates that the undoped 4H-SiC sample was successfully doped with boron and converted to p-type.

While performing laser doping, the substrate surface may be subject to damage caused by either the melting or ablation due to the heating effect of laser. Additionally, the agglomeration of dopant particulates on the substrate surface can also be a potential mechanism for damage. These processes can greatly affect the surface roughness and chemistry, making it imperative to address these concerns during the doping process. In our study, the surfaces of the undoped and boron-doped substrates were analyzed using a Bruker-DektakXT Stylus surface profilometer, as shown in Fig. 16. The laser-substrate interaction time was varied between 1 and 1.2 s, and the resulting surface profilometry outcomes have provided clear and noteworthy findings. Notably, the laser doping process did not cause any damage to the substrate surface. On the contrary, the surface smoothness was improved as the laser-substrate interaction time increased, which was evidenced in Fig. 16. Specifically, the average surface roughness (R_a) of the undoped sample decreased from 3.29 to 1.35 nm for the boron-doped sample with 1 s laser-substrate interaction time and 0.87 nm

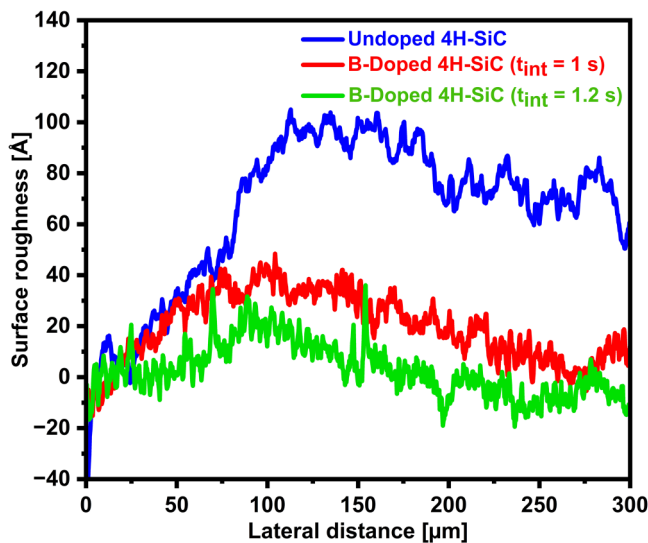


FIG. 16. Profilometry measurement of the surface roughness for the undoped and boron-doped substrates with laser-substrate interaction times of 1 and 1.2 s, respectively.

for the boron-doped sample with 1.2 s interaction time, indicating a significant improvement.

At the laser power of 30 W, the estimated temperatures on the substrate surface were 2662 and 2752 $^\circ\text{C}$ for the interaction times 1 and 1.2 s, respectively. For very tiny asperities on the rough surface of the original SiC wafer, the high temperatures could cause fusion and evaporation of the asperities and also tiny dopant particulates could agglomerate between two neighboring asperities.¹⁰ These physical phenomena could be the possible mechanisms for lower surface roughness at higher temperatures that occurred at higher interaction times. Additionally, the higher temperatures at higher interaction times could have caused more energetic phonons that induced the bonding of silicon and carbon atoms between two neighboring asperities, which could also be a possible mechanism for lower surface roughness at higher interaction times.

Laser doping enables the formation of localized heavily doped regions on semiconductors with many advantages such as (i) processing at ambient temperature, preventing high-temperature furnace annealing, and therefore, reducing the processing time;⁴ (ii) localized and selective energy transfer; and (iii) preventing the use of hazardous chemicals that are used in conventional doping.

VI. CONCLUSION

A laser doping technique based on a pulsed Nd:YAG laser (1064 nm) using a liquid-phase precursor of boron has been studied. The laser-assisted diffusion of boron dopant atoms into n-type 4H-SiC substrates to facilitate p-type doping is demonstrated. A theoretical model was employed in order to select laser processing parameters to maintain the temperature at the laser-substrate interaction zone well below the peritectic temperature of SiC during laser doping, thus preventing any damage, crystalline phase transitions in SiC, and minimizing the number of experiments. The 1064 nm laser heated up a localized volume of the SiC substrate (around the laser focal spot) to a very high temperature causing thermal decomposition of the precursor solution and enabling thermal diffusion of boron atoms into the SiC substrate. Additional vacancies in the SiC substrate were created by performing high power laser passes on the substrate prior to laser doping. FTIR spectrometry analysis revealed a reduction in transmittance and reflectance and an increase in absorbance of the doped 4H-SiC sample compared to the undoped sample. These results demonstrated the incorporation of boron atoms into the SiC substrate. Upon absorption of photons of $4.3\ \mu\text{m}$, the boron-doped 4H-SiC substrate experienced modifications in electron densities within its valence and acceptor energy levels. As a consequence, notable changes were detected in the absorption coefficient, absorption index, and refraction index of the doped 4H-SiC. Hence, the reflectivity of the SiC after doping was modified. Experimentally, a substantial variation in the refraction index of 0.356 was achieved after laser doping. The verification of p-type doping in 4H-SiC was confirmed by employing the hot point probe and photoluminescence techniques. Surface profilometry of the doped samples revealed that the laser doping process did not cause any damage to the substrate surface and the surface roughness decreased from 3.29 to 0.87 nm for the boron-doped sample when the interaction time was increased.

08 January 2024 14:36:20

ACKNOWLEDGMENTS

This work was supported by the Naval Air Warfare Center (NAWC), Aircraft Division under Contract No. N6833519P0493. The authors appreciate the Materials Characterization Facility (MCF) and the CREOL cleanroom at the University of Central Florida (UCF) and express their gratitude to Dowlat R. Sugrim for generously dedicating his time to create the 3D model of the experimental setup.

AUTHOR DECLARATIONS

Conflict of Interest

The authors have no conflicts to disclose.

Author Contributions

Gunjan Kulkarni: Conceptualization (equal); Data curation (equal); Formal analysis (equal); Investigation (equal); Methodology (equal); Software (equal); Validation (equal); Visualization (equal); Writing – original draft (equal); Writing – review & editing (equal). **Yahya Bougdid:** Conceptualization (equal); Data curation (equal); Formal analysis (equal); Investigation (equal); Validation (equal); Visualization (equal); Writing – original draft (equal); Writing – review & editing (equal). **Chandraika (John) Sugrim:** Funding acquisition (equal); Project administration (equal); Resources (equal); Writing – review & editing (equal). **Ranganathan Kumar:** Conceptualization (equal); Funding acquisition (equal); Investigation (equal); Methodology (equal); Project administration (equal); Resources (equal); Supervision (equal); Visualization (equal); Writing – review & editing (equal). **Aravinda Kar:** Conceptualization (equal); Funding acquisition (equal); Investigation (equal); Methodology (equal); Project administration (equal); Resources (equal); Supervision (equal); Validation (equal); Visualization (equal); Writing – review & editing (equal).

REFERENCES

- ¹Geunsik Lim, “An uncooled mid-wave infrared detector based on optical response of laser-doped silicon carbide,” Ph.D. thesis (University of Central Florida, Orlando, FL, 2014), <https://stars.library.ucf.edu/etd/4593>.
- ²G. Lim, T. Manzur, and A. Kar, “Optical response of laser-doped silicon carbide for an uncooled midwave infrared detector,” *Appl. Opt.* **50**, 2640–2653 (2011).
- ³Koji Nishi, Akihiro Ikeda, Hiroshi Ikenoue, and Tanemasa Asano, “Phosphorus doping into 4H-SiC by irradiation of excimer laser in phosphoric solution,” *Jpn. J. Appl. Phys.* **52**, 06GF02 (2013).
- ⁴Z. Tian, I. A. Salama, N. R. Quick, and A. Kar, “Effects of different laser sources and doping methods used to dope silicon carbide,” *Acta Mater.* **53**, 2835–2844 (2005).
- ⁵Evan M. Handy, Mulpuri V. Rao, O. W. Holland, P. H. Chi, K. A. Jones, M. A. Derenge, R. D. Vispute, and T. Venkatesan, “Al, B, and Ga ion-implantation doping of SiC,” *J. Electron. Mater.* **29**, 1340–1345 (2000).
- ⁶I. A. Salama, N. R. Quick, and A. Kar, “Laser doping of silicon carbide substrates,” *J. Electron. Mater.* **31**, 200–208 (2002).
- ⁷Sachin Bet, Nathaniel Quick, and Aravinda Kar, “Laser-doping of silicon carbide for p–n junction and LED fabrication,” *Phys. Status Solidi A* **204**, 1147–1157 (2007).
- ⁸Akihiro Ikeda, Koji Nishi, Hiroshi Ikenoue, and Tanemasa Asano, “Phosphorus doping of 4H SiC by liquid immersion excimer laser irradiation,” *Appl. Phys. Lett.* **102**, 052104 (2013).
- ⁹Daichi Marui, Akihiro Ikeda, Koji Nishi, Hiroshi Ikenoue, and Tanemasa Asano, “Aluminum doping of 4H-SiC by irradiation of excimer laser in aluminum chloride solution,” *Jpn. J. Appl. Phys.* **53**, 06JF03 (2014).
- ¹⁰Sachin Bet, “Laser enhanced doping for silicon carbide white light emitting diodes,” Ph.D. thesis (University of Central Florida, Orlando, FL, 2008), <https://stars.library.ucf.edu/etd/3680>.
- ¹¹Islam Abdel Haleem Salama, “Laser doping and metallization of wide bandgap materials: Silicon carbide, gallium nitride, and aluminum nitride,” Ph.D. dissertation, University of Central Florida, 2003.
- ¹²N. R. Quick, *Novel Techniques in Synthesis and Processing of Advanced Materials* (TMS, Warrendale, PA, 1994), pp. 419–432.
- ¹³N. R. Quick, in *Proceedings of International Conference on Lasers’94* (STS Press, McLean, VA, 1995), pp. 696–701.
- ¹⁴D. K. Sengupta, N. R. Quick, and A. Kar, “Laser conversion of electrical properties for silicon carbide device applications,” *J. Laser Appl.* **13**, 26–31 (2001).
- ¹⁵Geunsik Lim and Aravinda Kar, “Effects of laser scans on the diffusion depth and diffusivity of gallium in n-type 4H-SiC during laser doping,” *Mater. Sci. Eng. B* **176**, 660–668 (2011).
- ¹⁶Sachin Bet, Nathaniel Quick, and Aravinda Kar, “Effect of laser field and thermal stress on diffusion in laser doping of SiC,” *Acta Mater.* **55**, 6816–6824 (2007).
- ¹⁷Frank P. Incropera, David P. Dewitt, Theodore L. Bergman, and Adrienne S. Lavine, *Fundamentals of Heat and Mass Transfer. 2007* (John Wiley, Hoboken, NJ, 1985), pp. 939–940.
- ¹⁸Yahya Bougdid, Francois Chenard, John Sugrim, Ranganathan Kumar, and Aravinda Kar, “CO₂ laser-assisted sintering of TiO₂ nanoparticles for transparent films,” *J. Laser Appl.* **35**, 012012 (2023).
- ¹⁹Gady Golan, Alex Axelevitch, B. Gorenstein, and V. Manevych, “Hot-probe method for evaluation of impurities concentration in semiconductors,” *Microelectron. J.* **37**, 910–915 (2006).
- ²⁰A. Arvanitopoulos, N. Lophitis, S. Perkins, K. N. Gyftakis, M. B. Guadas, and M. Antoniou, “Physical parameterisation of 3C-silicon carbide (SiC) with scope to evaluate the suitability of the material for power diodes as an alternative to 4H-SiC,” in *2017 IEEE 11th International Symposium on Diagnostics for Electrical Machines, Power Electronics and Drives (SDEMPED)* (IEEE, New York, 2017), pp. 565–571.
- ²¹E. Hecht, *Optics* (Pearson Education India, Chennai, 2012); K. Racka, A. Avdonin, M. Sochacki, E. Tymicki, K. Graszka, R. Jakiela, B. Surma, and W. Dobrowolski, “Magnetic, optical and electrical characterization of SiC doped with scandium during the PVT growth,” *J. Cryst. Growth* **413**, 86–93 (2015).
- ²²J. Mazumder and A. Kar, *Theory and Application of Laser Chemical Vapor Deposition* (Springer Science & Business Media, New York, 2013).
- ²³N. Cherroret, A. Chakravarty, and A. Kar, “Temperature-dependent refractive index of semiconductors,” *J. Mater. Sci.* **43**, 1795–1801 (2008).
- ²⁴Okba Ben Khetta, Abdellah Attaf, Ammar Derbali, Hanane Saidi, Adel Bouhdjer, Mohamed Salah Aida, Youcef Ben Khetta, Radhia Messemeh, Rahima Nouadji, Saâd Rahmane, and Nour Elhouda Djehiche, “Precursor concentration effect on the physical properties of transparent titania (anatase-TiO₂) thin films grown by ultrasonic spray process for optoelectronics application,” *Opt. Mater.* **132**, 112790 (2022).
- ²⁵Michael Rubin, “Solar optical properties of windows,” *Int. J. Energy Res.* **6**, 123–133 (1982).
- ²⁶D. K. Schroder, *Semiconductor Material and Device Characterization* (John Wiley & Sons, New York, 2015).